ISSN (Online) 2287-3406
Journal of Life Science **2021** Vol. 31. No. 8. 719~728 DOI : https://doi.org/10.5352/JLS.2021.31.8.719

A Novel Synthesized Tyrosinase Inhibitor, (*E*)-3-(4-hydroxybenzylidene) chroman-4-one (MHY1294) Inhibits α-MSH-induced Melanogenesis in B16F10 Melanoma Cells

Hyeyoung Jeon, Seulah Lee, Seonguk Yang, EunJin Bang, Il Young Ryu, Yujin Park, Hee Jin Jung, Hae Young Chung, Hyung Ryong Moon* and Jaewon Lee*

College of Pharmacy, Pusan National University, Busan 46241, Korea

Received May 13, 2021 /Revised July 13, 2021 /Accepted July 29, 2021

Melanin pigments are abundantly distributed in mammalian skin, hair, eyes, and nervous system. Under normal physiological conditions, melanin protects the skin against various environmental stresses and acts as a physiological redox buffer to maintain homeostasis. However, abnormal melanin accumulation results in various hyperpigmentation conditions, such as chloasma, freckles, senile lentigo, and inflammatory pigmentation. Tyrosinase, a copper-containing enzyme, plays an important role in the regulation of the melanin pigment biosynthetic pathway. Although several whitening agents based on tyrosinase inhibition have been developed, their side effects, such as allergies, DNA damage, mutagenesis, and cytotoxicity of melanocytes, limit their applications. In this study, we synthesized 4-chromanone derivatives (MHY compounds) and investigated their ability to inhibit tyrosinase activity. Of these compounds, (E)-3-(4-hydroxybenzylidene)chroman-4-one (MHY1294) more potently inhibited the enzymatic activity of tyrosinase (IC_{50} = 5.1±0.86 μM) than kojic acid (14.3±1.43 μM), a representative tyrosinase inhibitor. In addition, MHY1294 showed competitive inhibitory action at the catalytic site of tyrosinase and had greater binding affinity at this site than kojic acid. Furthermore, MHY1294 effectively inhibited α-melanocyte stimulating hormone (α-MSH)-induced melanin synthesis and intracellular tyrosinase activity in B16F10 melanoma cells. The results of the present study indicate that MHY1294 may be considered as a candidate pharmacological agent and cosmetic whitening ingredient.

Key words : Anti-melanogenesis, B16F10 melanoma cells, kojic acid, MHY1294, tyrosinase inhibitor

Introduction

Melanin is the main pigment that determines the phenotypes of human skin and hair color. Studies have reported melanin has many properties, for example, it protects skin from UV-induced DNA damage and has antioxidant and anti-inflammatory effects [6, 30]. Because of these activities, melanin plays a critical role in the maintenance of healthy skin. On the other hand, under abnormal physiological conditions, melanin biosynthesis is not properly regulated and this can cause many serious facial esthetic and dermatological conditions such as chloasma, freckles, and senile lentigo, and dermatitis [1, 15].

Melanin is produced by epidermal melanocytes within cytoplasmic organelles called melanosomes, which are transferred to neighboring keratinocytes by melanocyte dendrites [14, 21]. Melanin biosynthesis is stimulated by biological factors such as α-melanocyte stimulating hormone (α-MSH), inflammatory cytokines, and growth factors, and chemical factors such as forskolin, 3-isobutyl-1-methylxanthine (IBMX), glycyrrhizin, and exposure to UV light [3, 9, 11]. During melanogenesis, the rate-limiting enzyme, tyrosinase, catalyzes two sequential reactions, that is, the hydroxylation of tyrosine to 3,4-dihydroxyphenylalanine (DOPA) and the dehydrogenation of DOPA to dopaquinone [13, 27]. Because tyrosinase is essential for melanogenesis, it has been considered a research target for potential inhibitors of melanin overproduction and most developed tyrosinase inhibitors are used to pharmaceuticals and cosmetics. Hydroquinone occurs naturally in leaves of blueberry, cranberry and bearberry plants and it has powerful tyrosinase inhibitory activity that has been conventionally used since the 1950s in skin-whitening agent [2, 28]. However, hydroquinone causes

***Corresponding authors**
Tel : +82-51-510-2815, Fax : +82-51-513-6754
E-mail : mhr108@pusan.ac.kr (Hyung Ryong Moon)
Tel : +82-51-510-2805, Fax : +82-51-513-6754
E-mail : neuron@pusan.ac.kr (Jaewon Lee)

skin irritation and is cytotoxic to melanocytes, and alternative agents are mainly used as skin whitening agents such as arbutin or kojic acid [10, 26]. These agents still have limitations as skin-whitening agents due to low solubility in oil, low stability at high temperature for long-term storage, and poor skin penetration [1, 7, 19]. Therefore, it remains a need for safe pharmacological and cosmetic agents of greater efficacy but with minimal adverse effects.

We previously synthesized thirteen (E)-benzylidene-1-indanone derivatives (BID1-13) and evaluated their activities, it demonstrated that BID3 have most effective tyrosinase inhibitory activity in B16F10 melanoma cells and have catalytic site of tyrosinase in silico molecular docking simulation, indicating possibility as whitening agent for the treatment of skin disorders [12]. Other researchers synthesized a series of homoisoflavonoids ((E)-3-benzylidenechroman-4-ones, 3-benzyl-4-H-chroman-4-ones, and 3-benzylchroman-4-ones) and demonstrated that (E)-3-benzylidenechroman-4-one derivatives have monoamine oxidase B inhibition activities in nano- or micromolar range [8]. Previously, we reported that (*E*)-β-phenyl-α,β-unsaturated carbonyl ((*E*)-PUSC) template plays an important role in exhibiting tyrosinase inhibitory activity [16]. Chromanone was considered the material for construction of the (*E*)-PUSC template. However, 2-chromanone and 3-chromanone were not suitable substances due to the formation of geometric isomers and the need for harsh conditions for the synthesis of this template, respectively. On the other hand, in the case of 4-chromanone, there was no such disadvantage. Therefore, 4-chromanone derivatives were designed as novel tyrosinase inhibitors. In the present study, we systematically designed and synthesized six 4-chromanone derivatives (MHY 1294-1299) produced by ring expansion into a 6-membered ring by adding an oxygen atom to the 5-membered ring fused with benzene and investigated the tyrosinase inhibitory activities of MHY compounds in B16F10 melanoma cells.

Materials and Methods

Reagents

Mushroom tyrosinase, L-tyrosine, L-DOPA (3,4-dihydroxyphenylalanine), kojic acid, α-melanocyte-stimulating hormone (α-MSH), paraformaldehyde (PFA), Triton-X 100, MTT [3-(4,5-dimethy1-2-thiazolyl)-2,5-diphenyl-2H-tetrazolium bromide], 4-Chromanone, benzaldehydes, and hydrogen chloride solution in 1M acetic acid were purchased from Sigma-Aldrich (St Louis, MO) and were used without further purification. Solvents including water, dichloromethane, ethyl acetate, hexane, and ethyl acetate were obtained from Daejung Chemicals (Seoul, Korea).

General procedure for the syntheses of MHY1294 -MHY1299

Reactions were monitored by thin-layer chromatography (TLC) on glass plates coated with silica gel using a fluorescent indicator (TLC Silica Gel 60 F254, Merck, Germany) and column chromatography was conducted on MP Silica 40-63, 60 Å. High resolution mass spectroscopy data was obtained on an Agilent Accurate Mass Q-TOF (quadruple-time of flight) liquid chromatography mass spectrometer (Agilent, Santa Clara, CA, USA) in negative ESI mode [8, 22]. Nuclear magnetic resonance (NMR) spectra were recorded on a Varian Unity INOVA 400 spectrometer at 400 MHz ^{1}H NMR, and on a Varian Unity INOVA 400 spectrometer for 100 MHz ^{13}C NMR. DMSO-δ6 (δH 2.50 ppm and δC 39.7 ppm) was used as solvents for NMR samples. Coupling constants (J) and chemical shifts (d) were measured in hertz (Hz) and parts per million (ppm), respectively. The abbreviations used for ^{1}H NMR data are; s (singlet), d (doublet), t (triplet), dd (doublet of doublets), and td (triplet of doublets).

To a mixture of 4-chromanone (100 mg, 0.67 mmol) and an appropriate substituted aldehyde (1.2 equiv.) was added 1M-HCl in acetic acid (0.4 ml). This mixture was then stirred at room temperature for 20-72 hr, water (5-10 ml) was added, and the reaction mixture was placed in a refrigerator overnight. The precipitate generated was filtered and washed with water, dichloromethane (DCM), ethyl acetate, hexane (Hx):dichloromethane (1:1), or hexane:ethyl acetate (EA) (1:1) (depending on the solubilities of residual raw materials and by-products) to give MHY1294 – MHY1299 as solids at yields of 24-60%. Washing solvent: H_2O, DCM and EA for MHY1294; H_2O and Hx/EA (1:1) for MHY1295 and MHY 1299; H_2O and Hx/DCM (1:1) for MHY1296, MHY1297, and MHY1298.

The *E*-/*Z*-configuration of the compounds was determined by vicinal ^{1}H, ^{13}C-coupling constants in proton- coupled ^{13}C spectra [31]. The ^{3}J values of the carbonyl carbon of the compounds showed roughly 6.4 Hz, implying that the compounds have an (*E*)-geometry.

(E)-3-(4-Hydroxybenzylidene)chroman-4-one (MHY 1294)

reaction time, 30 hr; yield, 24%; ^{1}H NMR (400 MHz,

DMSO-d_6) *d* 10.10 (s, 1 H, OH), 7.83 (d, 1 H, *J* = 8.0 Hz, 5-H), 7.64 (s, 1 H, vinylic H), 7.54 (t, 1 H, *J* = 7.6 Hz, 7-H), 7.30 (d, 2 H, *J* = 8.4 Hz, 2′-H, 6′-H), 7.08 (t, 1 H, *J* = 7.6 Hz, 6-H), 7.00 (d, 1 H, *J* = 8.4 Hz, 8-H), 6.84 (d, 2 H, *J* = 8.0 Hz, 3′-H, 5′-H), 5.39 (s, 2 H, 2-CH_2); ^{13}C NMR (100 MHz, DMSO-d_6) *d* 181.7, 161.1, 160.0, 137.6, 136.6, 133.5, 128.3, 127.8, 125.5, 122.5, 122.3, 118.5, 116.5, 68.2.

(E)-3-(3,4-Dihydroxybenzylidene)chroman-4-one (MHY1295)

reaction time, 20 hr; yield, 31%; ^{1}H NMR (400 MHz, DMSO-d_6) *d* 9.65 (s, 1 H, OH), 9.25 (s, 1 H, OH), 7.82 (dd, 1 H, *J* = 2.0, 8.0 Hz, 5-H), 7.56 (s, 1 H, vinylic H), 7.53 (td, 1 H, *J* = 2.0, 7.6 Hz, 7-H), 7.07 (t, 1 H, *J* = 8.0 Hz, 6-H), 7.00 (d, 1 H, *J* = 8.4 Hz, 8-H), 6.83 (s, 1 H, 2′-H), 6.81 (d, 1 H, *J* = 8.4 Hz, 6′-H), 6.77 (d, 1 H, *J* = 8.8 Hz, 5′-H), 5.38 (s, 2 H, 2-CH_2); ^{13}C NMR (100 MHz, DMSO-d_6) *d* 181.7, 161.1, 148.5, 146.1, 138.0, 136.6, 128.1, 127.8, 125.9, 124.2, 122.5, 122.3, 118.5, 118.4, 116.5, 68.2.

(E)-3-(4-Hydroxy-3-methoxybenzylidene)chroman-4-one (MHY1296)

reaction time, 45 hr; yield, 60%; ^{1}H NMR (400 MHz, DMSO-d_6) *d* 9.71 (s, 1 H, OH), 7.83 (dd, 1 H, *J* = 1.6, 7.6 Hz, 5-H), 7.66 (s, 1 H, vinylic H), 7.54 (td, 1 H, *J* = 1.6, 7.2 Hz, 7-H), 7.08 (t, 1 H, *J* = 7.2 Hz, 6-H), 7.02 (s, 1 H, 2′-H), 7.00 (d, 1 H, *J* = 8.4 Hz, 8-H), 6.88 (d, 1 H, *J* = 8.4 Hz, 6′-H), 6.85 (d, 1 H, *J* = 8.0 Hz, 5′-H), 5.42 (s, 2 H, 2-CH_2), 3.79 (s, 3 H, CH_3); ^{13}C NMR (100 MHz, DMSO-d_6) *d* 181.6, 161.1, 149.5, 148.3, 138.0, 136.6, 128.4, 127.9, 125.9, 125.2, 122.5, 122.3, 118.5, 116.4, 115.5, 68.3, 56.3.

(E)-3-(3-Hydroxy-4-methoxybenzylidene)chroman-4-one (MHY1297)

reaction time, 56 hr; yield, 43%; ^{1}H NMR (400 MHz, DMSO-d_6) *d* 9.29 (s, 1 H, OH), 7.83 (dd, 1 H, *J* = 1.6, 7.6 Hz, 5-H), 7.59 (s, 1 H, vinylic H), 7.54 (td, 1 H, *J* = 1.6, 8.4 Hz, 7-H), 7.08 (t, 1 H, *J* = 7.6 Hz, 6-H), 7.01 (s, 1 H, *J* = 8.4 Hz, 6′-H), 7.00 (d, 1 H, *J* = 8.0 Hz, 8-H), 6.88 (d, 1 H, *J* = 8.4 Hz, 5′-H), 6.87 (s, 1 H, 2′-H), 5.39 (s, 2 H, 2-CH_2), 3.80 (s, 3 H, CH_3); ^{13}C NMR (100 MHz, DMSO-d_6) *d* 181.7, 161.1, 150.1, 147.2, 137.6, 136.7, 129.0, 127.9, 127.3, 123.7, 122.5, 122.3, 118.5, 117.9, 112.7, 68.2, 56.3.

(E)-3-(4-Hydroxy-3,5-dimethoxybenzylidene)chroman-4-one (MHY1298)

reaction time, 48 hr; yield, 50%; ^{1}H NMR (400 MHz, DMSO-d_6) *d* 9.09 (s, 1 H, OH), 7.83 (d, 1 H, *J* = 7.6 Hz, 5-H), 7.66 (s, 1 H, vinylic H), 7.54 (t, 1 H, *J* = 8.0 Hz, 7-H), 7.08 (t, 1 H, *J* = 8.0 Hz, 6-H), 7.00 (d, 1 H, *J* = 8.4 Hz, 8-H), 6.71 (s, 2 H, 2′-H, 6′-H), 5.47 (s, 2 H, 2-CH_2), 3.78 (s, 6 H, 2×CH_3); ^{13}C NMR (100 MHz, DMSO-d_6) *d* 181.6, 161.1, 148.5, 138.7, 138.3, 136.6, 128.7, 127.9, 124.7, 122.5, 122.3, 118.5, 109.3, 68.3, 56.8.

(E)-3-(3-Bromo-4-hydroxybenzylidene)chroman-4-one (MHY1299)

reaction time, 3 day; yield, 46%; melting point: 177.3 - 178.5 ℃; ^{1}H NMR (400 MHz, DMSO-d_6) *d* 10.92 (s, 1 H, OH), 7.82 (dd, 1 H, *J* = 2.0, 8.0 Hz, 5-H), 7.62 (d, 1 H, *J* = 2.0 Hz, 2′-H), 7.60 (s, 1 H, vinylic H), 7.54 (td, 1 H, *J* = 2.0, 7.6 Hz, 7-H), 7.27 (dd, 1 H, *J* = 2.0, 8.4 Hz, 6′-H), 7.08 (t, 1 H, *J* = 8.0 Hz, 6-H), 7.02 (d, 1 H, *J* = 8.4 Hz, 5′-H), 7.01 (d, 1 H, *J* = 8.4 Hz, 8-H), 5.37 (s, 2 H, 2-CH_2); ^{13}C NMR (100 MHz, DMSO-d_6) *d* 181.6, 161.2, 156.4, 136.8, 136.1, 136.1, 132.0, 129.6, 127.9, 127.1, 122.6, 122.2, 118.5, 117.1, 110.4, 68.1.; HRMS (ESI-) *m/z* $C_{16}H_{11}BrO_3$ $(M-H)^-$ calcd 328.9819, obsd 328.9819, $(M-H+2)^-$ calcd 330.9800, obsd 330.9803.

Mushroom tyrosinase inhibitory activity assay

Purified mushroom tyrosinase was used as the target enzyme to evaluate the inhibitory effect of tyrosinase, which was determined spectrophotometrically by measuring the conversion of L-tyrosine to DOPAchrome, as previously described with some modification [25]. In brief, 20 µl aliquots of aqueous mushroom tyrosinase solution (500 units/ml) were placed in the wells of 96-well plates in a total assay volume of 200 µl. The assay mixture buffer contained 1 mM L-tyrosine, 50 mM sodium phosphate buffer (pH 6.5, mixing 50 mM monobasic and 50 mM dibasic forms of sodium phosphate to give the correct pH), and purified water in a 10:10:9 ratio. The reaction mixture was incubated at 37℃ for 20 min and DOPAchrome concentrations were monitored by measuring absorbance at 450 nm using an ELISA microplate reader. The tyrosinase activity of MHY series (40 µM) and kojic acid (40 µM) was screened and kojic acid used as the reference tyrosinase inhibitor. Tyrosinase inhibitory activities (%) were calculated using: {1 - (Abssample-Abscontrol) / Abscontrol} ×100. Dose-dependent inhibition experiments were performed in triplicate to determine the half-maximal (50%) inhibitory concentrations (IC_{50} values).

Kinetic analysis of tyrosinase inhibitory activity

To investigate the kinetic mechanism of tyrosinase inhibition, we used Lineweaver-Burk plots. Briefly, various concentrations of L-tyrosine (0.25, 0.5, 1, 2, or 4 mM), 20 µl

aqueous solution of tyrosinase (1,000 units/ml) isolated from mushrooms, 50 mM potassium phosphate buffer (pH 6.5), and different concentrations of MHY1294 (0, 5, 10, or 20 μM) were placed in a 96-well plate in a total volume of 200 μl. Rates of DOPAchrome formation in reaction mixtures were measured by absorbance at 450 nm per min (ΔOD_{450}/min) using a microplate reader. To investigated the inhibitory mechanism, we used Lineweaver-Burk double reciprocal plots [a plot of 1/reaction velocity (1/V) vs. 1/substrate concentration (1/[S])]. Michalis constants (K_m) and maximum velocity (V_{max}) of tyrosinase were obtained using Lineweaver-Burk plots at various concentrations of L-tyrosine. Dixon plot is plotted the 1/V against the inhibitor (MHY1294) concentrations and three concentrations of L-tyrosine, the K_i values was determined at one point in the fourth quadrant of each slope lines of L-tyrosine concentration.

Docking simulation of tyrosinase inhibition

Energies of MHY1294 or kojic acid to tyrosinase bindings were determined as previously described with slight modification [23, 24, 32]. Chem3D Pro 12.0 software was used to create 3D structures of MHY1294 or kojic acid and the 3D structure of Agaricus bisporus tyrosinase was imported from Protein Data Bank (PDB) (ID: 2Y9X). Docking scores between MHY1294 or kojic acid and tyrosinase were calculated using AutoDock Vina 1.1.2 and Chimera software. LigandScout 4.3 was used to generating pharmacophore models of interactions between MHY1294 or kojic acid and the amino acid residues of tyrosinase.

Cell culture

B16F10 cells (a murine melanoma cell line) were purchased from the American Type Culture Collection (Manassas, VA, USA) and maintained in culture plates in Dulbecco's modified Eagle's medium (DMEM, Welgene, Daegu, South Korea) supplemented with 5% (v/v) fetal bovine serum (FBS), 1% (v/v) penicillin-streptomycin in a humidified 5% CO_2/95%

Cell viability assay

The effect of MHY1294 on B16F10 cell viability was determined using an MTT (3-(4,5-dimethylthiazol-2-yl)-2,5-diphenyltetrazolium bromide) assay. Cells were plated in 96-well plate at a density of 3×10^3 cells/well and incubated in a humidified 5% CO_2/95% air atmosphere at 37℃ for 24 hr when culture medium was replaced with fresh medium containing different concentrations of MHY1294 (0.5, 1, 2, 5, or 10 μM). Cells were then incubated for up to 72 hr, media were removed, and 200 μl of MTT solution (0.5 mg/ml in PBS) was added to each well. Cells were then incubated at 37℃ for 4 hr, supernatants were discarded, and formazan crystals in viable cells were dissolved using solubilization solution (DMSO:ethanol 1:1 v/v). Formazan absorbances were determined using an ELISA microplate reader at 560 nm.

Assessment of melanin contents

Levels of intracellular and secreted melanin were measured, as previously described with slight modification [5]. B16F10 cells (1×10^5 cells/ml) were seeded in 60-mm dishes and left to grow overnight in a humidified CO_2/95% air atmosphere at 37℃. The culture medium was then replaced with phenol red-free DMEM containing MHY1294 (1 or 10 μM) or kojic acid (50 μM) and stimulated with 2 μM α-MSH for 96 hr. Cultured cells and media were then harvested. Cell pellets were dissolved in 100 μl of 1 N NaOH containing 5% DMSO by boiling at 60℃ for 1 hr. Melanin levels were determined by measuring absorbances using a microplate reader at 405 nm.

In situ intracellular tyrosinase activity assay

In situ intracellular tyrosinase activity was assessed using a previously described method with slight modification [18]. B16F10 cells (10×10^4 cells/ml) were seeded in 60-mm dishes and allowed to attach overnight in a humidified 5% CO_2/95% air atmosphere at 37℃. Different concentrations of MHY1294 (1 or 10 μM) and kojic acid (50 μM) were added to the cultured cells, which were then stimulated with 2 μM α-MSH for 48 hr. Cells were then fixed using 4% paraformaldehyde (PFA) in PBS for 40 min at room temperature, the fixative was aspirated, cells were washed with PBS, and permeabilized for 2 min in 0.1% Triton X-100. After thorough washing with PBS, cells were reacted with 2 mM L-DOPA for 2 hr at 37℃ and rinsed with PBS. Stained cells were imaged and observed under a Nikon ECLIPSE TE 2000-U microscope (Nikon, Tokyo, Japan).

Statistical analysis

The significances of intergroup differences were determined by one-way analysis of variance (ANOVA) with Fisher's protected least significant difference (PLSD) test. The analysis was performed using Statview software (Ver-

Table 1. The chemical structures of (E)-3-(substituted benzylidene)chroman-4-one derivatives

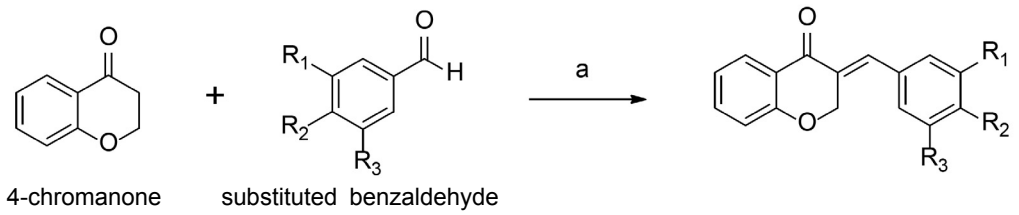

4-chromanone substituted benzaldehyde

Compounds	R_1	R_2	R_3
MHY1294	H	OH	H
MHY1295	OH	OH	H
MHY1296	OMe	OH	H
MHY1297	OH	OMe	H
MHY1298	OMe	OH	OMe
MHY1290	Br	OH	H

sion 5.0.1., SAS Institute Inc., Cary, NC, USA), and P values of < 0.05 were considered to indicate significance.

Results and Discussion

Tyrosinase inhibitory activity of synthesized 4-chromanone derivatives

Tyrosinase is central to the biosynthetic pathway leading to melanin formation. Accordingly, the investigation of tyrosinase inhibition activity has been considered an important indicator evaluating the efficacy of numerous skin whitening compounds [4, 17, 20]. In the present study, we synthesized 4-chromanone derivatives according to the general Table 1. Then, we investigated the tyrosinase inhibitory potential of 4-chromanone derivatives using mushroom tyrosinase in a cell-free *in vitro* system and L-tyrosine as substrate. Of these compounds, 40 μM of MHY1294 and MHY1297 more potently inhibited mushroom tyrosinase activity with 94.7±0.39% and 98.6±0.34% respectively, compared with the positive control kojic acid which has the value of 93.0±1.70% (Table 2). Next, we evaluated concentration-dependent tyrosinase inhibitory activity to measure IC_{50} values, and only used MHY1294 in detail because MHY1294 was not cytotoxic up to 10 μM, whereas MHY1297 significantly decreased cell viability at $\geq$1 μM, indicating cytotoxicity in B16F10 melanoma cells (data not shown). MHY1294 exhibited an IC_{50} value of 5.1±0.86 μM which has stronger inhibitory activity than kojic acid with IC_{50} value of 14.3±1.43 μM (Table 3). Therefore, MHY1294 was found to be more effective at inhibiting tyrosinase activity than kojic acid, a well-known whitening agent.

Table 2. The inhibitory activities of 4-chromanone derivatives and kojic acid against mushroom tyrosinase

Compounds	Tyrosinase inhibition activity (%)
MHY1294	94.7±0.39
MHY1295	60.7±1.22
MHY1296	32.3±0.79
MHY1297	98.6±0.34
MHY1298	16.8±3.41
MHY1299	57.9±1.31
Kojic acid	93.0±1.70

Tyrosinase inhibitory activities of synthesized compounds (40 μM) were evaluated using L-tyrosine as a substrate. Results are expressed as means ± standard errors (n=4).

Enzyme kinetic analysis of MHY1294 on tyrosinase inhibition activity

In order to investigate how MHY1294 affect the enzyme kinetics of tyrosinase, two complementary kinetic analysis

Table 3. IC_{50} values for the inhibition of mushroom tyrosinase by MHY1294 or kojic acid

Compounds	Concentration (μM)	Inhibition (%)	IC_{50} (μM)
Kojic acid	2.5	14.4±2.12	14.3±1.43
	5	36.4±2.43	
	10	57.2±1.66	
	20	79.2±2.45	
MHY1294	2.5	36.5±3.13	5.1±0.86**
	5	45.2±2.40	
	10	69.5±3.63	
	20	83.9±2.26	

IC_{50} (half-maximal inhibitory concentration) values were obtained on Lineweaver-Burk plot using L-tyrosine as a substrate. Results are expressed as means ± standard errors (n=3).

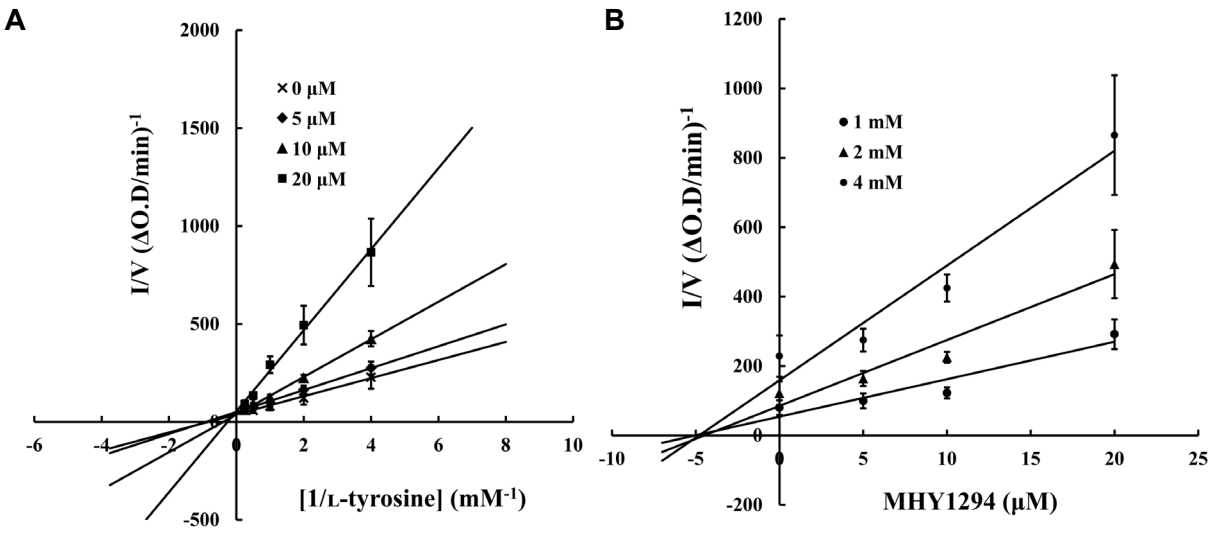

C

Compound	Concentration (μM)	V_{max} (mM/min)	K_m (mM)
MHY1294	0	3.0×10^{-2}	0.98
	5	3.0×10^{-2}	1.53
	10	3.0×10^{-2}	2.70
	20	3.0×10^{-2}	7.25

Fig. 1. Lineweaver-Burk plot for the inhibition of mushroom tyrosinase by MHY1294. (A) Lineweaver-Burk plots were constructed by plotting mean 1/V (the inverse of reaction velocity) vs. 1/[S] (the inverse of substrate concentration). (B) Dixon plots were constructed by plotting means of 1/V vs 1/[MHY1294]. Results are expressed as means ± standard errors (n=3). (C) Results are presented as mean 1/V values, that is, as the inverse of absorbance increases per minute at 450 nm (ΔA450/min). The equation of the Lineweaver-Burk plot is: $1/V = K_m/V_{max} \times 1/[S] + 1/V_{max}$. Where V is reaction velocity, K_m is the Michaelis-Menten constant, V_{max} is maximum reaction velocity, and [S] is substrate concentration.

were performed using various concentration of L-tyrosine and MHY1294. Lineweaver-Burk double-reciprocal plots revealed four distinct slopes, which intersected at one point on the y-axis, indicating MHY1294 inhibited tyrosinase in a competitive manner (Fig. 1A). Dixon plot is well known to determine Ki value that extrapolated lines of different substrate concentrations intersect at one point in competitive inhibition [33]. Dixon plot analysis confirmed that MHY1294 competitively inhibit tyrosinase activity and Ki value was 5.25 μM for L-tyrosine substrate (Fig. 1B). The Km values of MHY1294 at concentrations of 0, 5, 10, and 20 μM for tyrosinase were 0.98, 1.53, 2.70, and 7.25 mM, respectively, and Vmax values remained constant (3.0×10^{-2} mM/min) (Fig. 1C). Therefore, this result confirmed that MHY1294 has an inhibitory effect of tyrosinase activity through competitive inhibition, and it was also assumed that MHY1294 binds to the active site of tyrosinase.

Docking simulation of MHY1294

Based on kinetic results, we examined the molecular mechanism underlying tyrosinase inhibition by MHY1294 using docking simulation. Interestingly, this results showed that MHY1294 interacted hydrophobically with three tyrosinase residues, namely, VAL283, ALA286, and PHE264 (Fig. 2A, Fig. 2C), and that kojic acid interacted by hydrogen bonding with HIS259, HIS263, and MET280 (Fig. 2B, Fig. 2D). In addition, the obtained docking scores provide a useful means of evaluating binding affinities between enzymes and their substrates. The binding energy of tyrosinase and MHY1294 (-7.4 kcal/mol) was greater than tyrosinase/kojic acid (-5.7 kcal/mol), suggesting MHY1294 could be superior to kojic acid in competitive binding with tyrosinase (Fig. 2E). This finding implied that MHY1294 bound non-covalently to amino acid residues at the active site of tyrosinase indicating that MHY1294 is a competitive inhibitor of tyrosinase.

MHY1294 attenuated α-MSH-induced melanin synthesis and intracellular tyrosinase activity in B16F10 melanoma cells without affecting cell viability

Skin-whitening agents that suppress tyrosinase must penetrate melanocyte cell membranes [29], and thus, we inves-

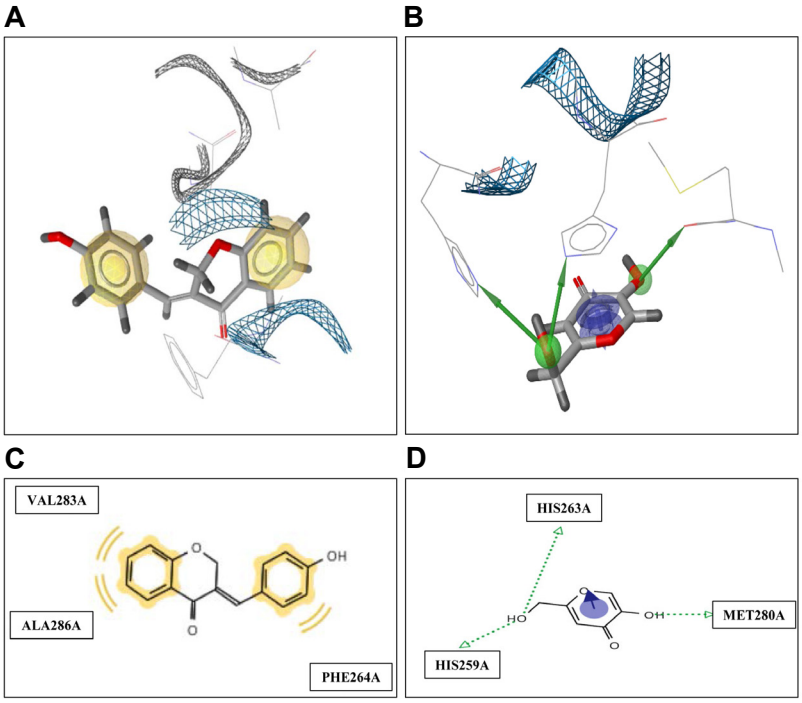

E

Compounds	Docking score (kcal/mol)
MHY1294	-7.4
Kojic acid	-5.7

Fig. 2. Molecular docking simulation between mushroom tyrosinase and MHY1294 or kojic acid. Docking simulation was performed to predict binding dispositions and binding affinities. Computation provided docking simulation images for (A) MHY1294 and (B) kojic acid with mushroom tyrosinase. The residues of (C) MHY1294 and (D) kojic acid that interact with tyrosinase were identified using LigandScout. The Protein Data Bank (PDB) code of mushroom tyrosinase is 2Y9X. (E) The docking scores indicated binding affinities between MHY1294 or kojic acid and the catalytic site of tyrosinase.

tigated the anti-melanogenic effect of MHY1294 on B16F10 murine melanoma cells. As a first step toward determining the pharmacological effect of MHY1294 on melanin synthesis induced by α-MSH, we investigated the cytotoxic effect of MHY1294 on B16F10 melanoma cells. MHY1294 at 0.5, 1, 2, 5, and 10 μM did not affect cell viability on B16F10 melanoma after 72 hr, indicating that up to 10 μM of MHY1294 is considered as a safe concentration range for the evaluation of tyrosinase inhibitory activity in vitro (Fig. 3A). In order to determine the inhibitory effect of MHY1294 on melanin production, we quantified melanin contents in α-MSH-induced B16F10 melanoma cells treated with MHY 1294 or kojic acid for 96 hr. Levels of melanin were measured at both the extracellular content (released into the medium) and intracellular content (accumulated in pellets of B16F10 melanoma cells). MHY1294 decreased melanin pigmentation extra- and intracellularly (Fig. 3B, Fig. 3C). When we measured the effect of MHY1294 on intracellular tyrosinase activity, we found that MHY1294 suppressed α-MSH-induced intracellular tyrosinase activation in B16F10 cells (Fig. 3D), which was in line with our cell-free in vitro data and indicated MHY1294 directly inhibited tyrosinase activity. These results demonstrate that MHY1294 suppressed α-MSH-stimulated melanin production and intracellular tyrosinase activity in B16F10 melanoma cells without any cytotoxic effect. In conclusion, MHY1294 was found to possess anti-melanogenic effects in B16F10 melanoma cells and these were attributed to the suppression of tyrosinase activation. However, MHY1294 did not affect cell viability. Furthermore, our results indicate that the depigmenting effect of MHY1294 is due to the direct inhibition of tyrosinase activity. These findings suggest MHY1294 be viewed as a candidate for treating skin hyperpigmentation disorders and as a cosmetic whitening agent.

Acknowledgement

This work was supported by a 2-Year Research Grant from Pusan National University.

The Conflict of Interest Statement

The authors declare that they have no conflicts of interest with the contents of this article.

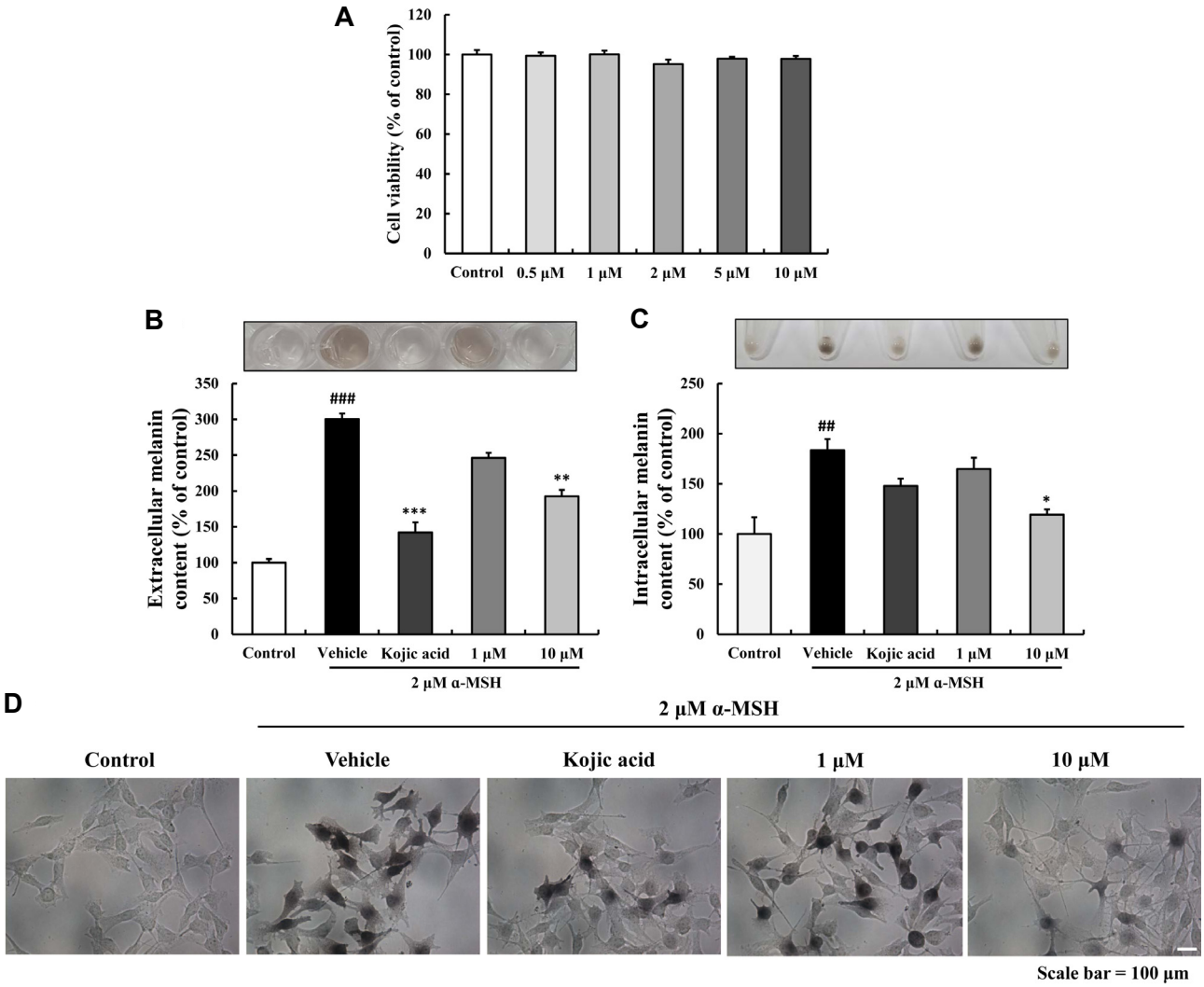

Fig. 3. MHY1294 inhibited α-MSH-induced melanization and intracellular tyrosinase activation in B16F10 melanoma cells. (A) Cells were treated with different concentrations of MHY1294 (0.5, 1, 2, 5, or 10 μM) for 72 hr. Cell viability was evaluated using an MTT assay. Results are expressed as means ± standard errors (n=8). (B) Extracellular and (C) intracellular melanin contents. Results are expressed as means ± standard errors (n=3). * $p<0.05$ vs. α-MSH-treated controls, # $p<0.05$ vs controls. (D) *In situ* intracellular tyrosinase activities were determined as described in Materials and Methods section. Representative images were captured under a Nikon ECLIPSE TE 2000-U microscope (Nikon, Tokyo). Scale bar = 100 μm.

References

1. Alam, M. B., Ahmed, A., Motin, M. A., Kim, S. and Lee, S. H. 2018. Attenuation of melanogenesis by Nymphaea nouchali (Burm. f) flower extract through the regulation of cAMP/ CREB/MAPKs/MITF and proteasomal degradation of tyrosinase. *Sci. Rep.* **8**, 1-14.
2. Arndt, K. A. and Fitzpatrick, T. B. 1965. Topical use of hydroquinone as a depigmenting agent. *JAMA*. **194**, 965-967.
3. Balcos, M. C., Kim, S. Y., Jeong, H. S., Yun, H. Y., Baek, K. J., Kwon, N. S., Park, K. C. and Kim, D. S. 2014. Docosahexaenoic acid inhibits melanin synthesis in murine melanoma cells in vitro through increasing tyrosinase degradation. *Acta. Pharmacol. Sin.* **35**, 489-495.
4. Bang, E., Noh, S. G., Ha, S., Jung, H. J., Kim, D. H., Lee, A. K., Hyun, M. K., Kang, D., Lee, S. and Park, C. 2018. Evaluation of the novel synthetic tyrosinase inhibitor (Z)-3-(3-bromo-4-hydroxybenzylidene) thiochroman-4-one (MHY 1498) *in vitro* and *in silico*. *Molecules* **23**, 3307.
5. Bilodeau, M. L., Greulich, J. D., Hullinger, R. L., Bertolotto, C., Ballotti, R. and Andrisani, O. M. 2001. BMP-2 stimulates tyrosinase gene expression and melanogenesis in differentiated melanocytes. *Pigment Cell Res.* **14**, 328-336.
6. Brenner, M. and Hearing, V. J. 2008. The protective role of melanin against UV damage in human skin. *Photochem. Photobiol.* **84**, 539-549.
7. Chen, W. C., Tseng, T. S., Hsiao, N. W., Lin, Y. L., Wen, Z. H., Tsai, C. C., Lee, Y. C., Lin, H. H. and Tsai, K. C.

2015. Discovery of highly potent tyrosinase inhibitor, T1, with significant anti-melanogenesis ability by zebrafish in vivo assay and computational molecular modeling. *Sci. Rep.* **5**, 7995.
8. Desideri, N., Bolasco, A., Fioravanti, R., Monaco, L. P., Orallo, F., Yanez, M., Ortuso, F. and Alcaro, S. 2011. Homoisoflavonoids: Natural scaffolds with potent and selective monoamine oxidase-B inhibition properties. *J. Med. Chem.* **54**, 2155-2164.
9. Halaban, R., Pomerantz, S. H., Marshall, S. and Lerner, A. B. 1984. Tyrosinase activity and abundance in Cloudman melanoma cells. *Arch. Biochem. Biophys.* **230**, 383-387.
10. Hu, Z. M., Zhou, Q., Lei, T. C., Ding, S. F. and Xu, S. Z. 2009. Effects of hydroquinone and its glucoside derivatives on melanogenesis and antioxidation: Biosafety as skin whitening agents. *J. Dermatol. Sci.* **55**, 179-184.
11. Hunt, G., Todd, C., Cresswell, J. E. and Thody, A. J. 1994. Alpha-melanocyte stimulating hormone and its analogue Nle4DPhe7 alpha-MSH affect morphology, tyrosinase activity and melanogenesis in cultured human melanocytes. *J. Cell. Sci.* **107**, 205-211.
12. Jung, H. J., Noh, S. G., Park, Y., Kang, D., Chun, P., Chung, H. Y. and Moon, H. R. 2019. *In vitro* and in silico insights into tyrosinase inhibitors with (E)-benzylidene-1-indanone derivatives. *Comput. Struct. Biotechnol. J.* **17**, 1255-1264.
13. Kang, S. J., Choi, B. R., Lee, E. K., Kim, S. H., Yi, H. Y., Park, H. R., Song, C. H., Lee, Y. J. and Ku, S. K. 2015. Inhibitory effect of dried pomegranate concentration powder on melanogenesis in B16F10 melanoma cells; involvement of p38 and PKA signaling pathways. *Int. J. Mol. Sci.* **16**, 24219-24242.
14. Kim, A., Yim, N. H., Im, M., Jung, Y. P., Liang, C., Cho, W. K. and Ma, J. Y. 2013. Ssanghwatang, an oriental herbal cocktail, exerts anti-melanogenic activity by suppression of the p38 MAPK and PKA signaling pathways in B16F10 cells. *BMC. Complement. Altern. Med.* **13**, 214.
15. Kim, C. S., Noh, S. G., Park, Y., Kang, D., Chun, P., Chung, H. Y., Jung, H. J. and Moon, H. R. 2018. A potent tyrosinase inhibitor,(E)-3-(2, 4-dihydroxyphenyl)-1-(thiophen-2-yl) prop-2-en-1-one, with anti-melanogenesis properties in α-MSH and IBMX-induced B16F10 melanoma cells. *Molecules* **23**, 2725.
16. Kim, H. R., Lee, H. J., Choi, Y. J., Park, Y. J., Woo, Y., Kim, S. J., Park, M. H., Lee, H. W., Chun, P., Chung, H. Y. and Moon, H. R. 2014. Benzylidene-linked thiohydantoin derivatives as inhibitors of tyrosinase and melanogenesis: importance of the β-phenyl-α,β-unsaturated carbonyl functionality. *Med. Chem. Commun.* **5**, 1410.
17. Kim, S. H., Ha, Y. M., Moon, K. M., Choi, Y. J., Park, Y. J., Jeong, H. O., Chung, K. W., Lee, H. J., Chun, P. and Moon, H. R. 2013. Anti-melanogenic effect of (Z)-5-(2,4-dihydroxybenzylidene) thiazolidine-2,4-dione, a novel tyrosinase inhibitor. *Arch. Pharm. Res.* **36**, 1189-1197.
18. Ko, G. A. and Kim Cho, S. 2018. Ethyl linoleate inhibits α-MSH-induced melanogenesis through Akt/GSK3β/β-catenin signal pathway. *Kor. J. Physiol. Pharmacol.* **22**, 53-61.
19. Lajis, A. F., Hamid, M. and Ariff, A. B. 2012. Depigmenting effect of kojic acid esters in hyperpigmented B16F1 melanoma cells. *J. Biomed. Biotechnol.* **2012,** doi:10.1155/2012/952452.
20. Lee, S. E., Park, S. H., Oh, S. W., Yoo, J. A., Kwon, K., Park, S. J., Kim, J., Lee, H. S., Cho, J. Y. and Lee, J. 2018. Beauvericin inhibits melanogenesis by regulating cAMP/PKA/CREB and LXR-α/p38 MAPK‐mediated pathways. *Sci. Rep.* **8**, 1-12.
21. Lim, J. W., Ha, J. H., Jeong, Y. J. and Park, S. N. 2018. Anti-melanogenesis effect of dehydroglyasperin C through the downregulation of MITF via the reduction of intracellular cAMP and acceleration of ERK activation in B16F1 melanoma cells. *Pharmacol. Rep.* **70**, 930-935.
22. Liu, Q. H., Wu, J. J., Li, F., Cai, P., Yang, X. L., Kong, L. Y. and Wang, X. B. 2017. Synthesis and pharmacological evaluation of multi-functional homoisoflavonoid derivatives as potent inhibitors of monoamine oxidase B and cholinesterase for the treatment of Alzheimer's disease. *Med. Chem. Commun.* **8**, 1459-1467.
23. Morris, G. M., Goodsell, D. S., Halliday, R. S., Huey, R., Hart, W. E., Belew, R. K. and Olson, A. J. 1998. Automated docking using a Lamarckian genetic algorithm and an empirical binding free energy function. *J. Comput. Chem.* **19**, 1639-1662.
24. Moustakas, D. T., Lang, P. T., Pegg, S., Pettersen, E., Kuntz, I. D., Brooijmans, N. and Rizzo, R. C. 2006. Development and validation of a modular, extensible docking program: DOCK 5. *J. Comput. Aided. Mol. Des.* **20**, 601-619.
25. No, J. K., Kim, Y. J., Shim, K. H., Jun, Y. S., Rhee, S. H., Yokozawa, T. and Chung, H. Y. 1999. Inhibition of tyrosinase by green tea components. *Life Sci.* **65**, PL241-PL246.
26. O'Donoghue, J. L. 2006. Hydroquinone and its analogues in dermatology-a risk benefit viewpoint. *J. Cosmet. Dermatol.* **5**, 196-203.
27. Oh, T. I., Yun, J. M., Park, E. J., Kim, Y. S., Lee, Y. M. and Lim, J. H. 2017. Plumbagin suppresses α-MSH-induced melanogenesis in B16F10 mouse melanoma cells by inhibiting tyrosinase activity. *Int. J. Mol. Sci.* **18**, 320.
28. Parvez, S., Kang, M., Chung, H. S., Cho, C., Hong, M. C., Shin, M. K. and Bae, H. 2006. Survey and mechanism of skin depigmenting and lightening agents. *Phytother. Res.* **20**, 921-934.
29. Petit, L. and Pierard, G. 2003. Skin lightening products revisited. *Int. J. Cosmet. Sci.* **25**, 169-181.
30. Suwannarach, N., Kumla, J., Watanabe, B., Matsui, K. and Lumyong, S. 2019. Characterization of melanin and optimal conditions for pigment production by an endophytic fungus, Spissiomyces endophytica SDBR-CMU319. *PloS One* **14**, e0222187.
31. Vogeli, U., von Philipsborn, W., Nagarajan, K. and Nair, M. D. 1978. Structure of addition products of acetylenedicarboxylic acid esters with various dinucleophiles. An application of C, H-spin-coupling constants. *Helvetica. Chimica. Acta.* **61**, 607-617.

32. Wolber, G. and Langer, T. 2005. LigandScout: 3-D Pharmacophores derived from protein-bound ligands and their use as virtual screening filters. *J. Chem. Inf. Model.* **45**, 160-169.

33. Yoshino, M. and Murakami, K. 2009. A graphical method for determining inhibition constants. *J. Enzyme Inhib. Med. Chem.* **24**, 1288-1290.

초록 : 신규 합성물질 (*E*)-3-(4-하이드록시벤질리딘)크로마논 유도체의 티로시나아제 효소활성 저해 및 멜라닌 생성 억제 효과

전혜영 · 이슬아 · 양성욱 · 방은진 · 유일영 · 박유진 · 정희진 · 정해영 · 문형룡* · 이재원*
(부산대학교 약학대학 약학과)

멜라닌 색소는 포유동물의 피부, 머리카락, 눈, 신경계에 풍부하게 존재한다. 멜라닌은 다양한 환경적 스트레스로부터 피부를 보호하며, 생리학적 산화-환원 완충 작용을 통해 항상성을 유지한다. 그러나, 과도한 멜라닌 축적은 간반, 주근깨, 노인성 흑자, 염증성 색소침착을 일으킬 수 있다. 티로시나아제는 멜라닌의 생합성 경로 조절에 아주 중요한 역할을 하는 것으로 알려져 있다. 티로시나아제의 활성을 저해하는 다양한 미백제가 개발되었지만 알러지, DNA손상, 세포독성, 돌연변이 유발 등을 야기하는 부작용으로 인해 임상적 적용이 제한되었다. 본 논문에서 여러 4-크로마논 유도체를 합성하여 티로시나아제 억제 활성을 조사하였다. 이들 화합물 중 MHY1294는 IC_{50}가 5.1±0.86 μM으로 양성 대조군인 코직산(14.3±1.43 μM) 보다 나은 티로시나아제 효소 억제 활성을 나타냈다. 또한 MHY1294는 티로시나아제의 촉매 부위에서 경쟁적인 억제 작용을 보였으며 코직산보다 더 큰 기질 결합 친화성을 가지는 것으로 확인되었다. 뿐만 아니라, MHY1294는 B16F10 흑색종 세포에서 멜라닌 세포 자극 호르몬(α-MSH)에 의해 유도되는 멜라닌 합성과 세포 내 티로시나아제 활성을 유의적으로 억제하였다. 결론적으로 본 연구는 MHY1294가 과도한 멜라닌 축적에 대한 약물 제제 및 미백제로서의 개발 가능성이 있음을 시사한다.